BL19B2
Engineering Science Research I

1. Introduction

BL19B2 is a bending magnet beamline dedicated to X-ray diffraction and scattering experiments for the industrial use of synchrotron radiation. To meet the diverse needs of the industry, various experimental apparatuses are provided in this beamline. In the first hutch (EH1) and second hutch (EH2), a versatile high-throughput powder diffractometer, *Polaris*, and a multi-axis diffractometer are installed, respectively. In the third hutch (EH3), an apparatus for small-angle X-ray scattering (SAXS) with a camera length of 0.7–3 m is installed. The detector of this apparatus is a two-dimensional detector, PILATUS 2M. Furthermore, an apparatus for ultrasmall-angle X-ray scattering (USAXS) with a camera length of 41 m is provided by setting the sample stage in EH2 and utilizing PILATUS 2M in EH3 as the detector. In FY2021, the detector system of the multi-axis diffractometer was upgraded. For USAXS, the optical setup was significantly improved. In addition, a device controlling the temperature of samples for SAXS/USAXS measurement was installed.

2. Upgrade of scintillation detector system of multi-axis diffractometer

The multi-axis diffractometer installed in EH2 is widely used by engineering science researchers. In FY2022, we newly introduced a new scintillation detector (C30LaBr25B, $LaBr_3:Ce^{3+}$), preamplifier (CP-10A), and pulse processor (C400). The decay time of the $LaBr_3:Ce^{3+}$ scintillator is 16 ns. It is shorter than that of NaI:Tl, which is the conventional scintillator we have used. Therefore, it was expected that the dynamic range of detecting X-ray diffraction signals with a high counting rate was improved using this new detector system.

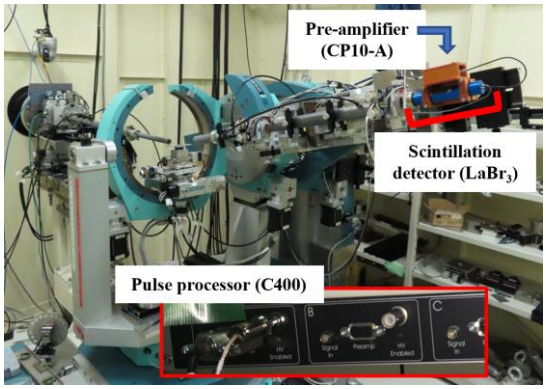

Fig. 1. Schematic photograph of a $LaBr_3:Ce^{3+}$ scintillator and preamplifier attached to a multi-axis diffractometer.

Figure 1 shows a schematic photograph of a $LaBr_3:Ce^{3+}$ scintillation detector and preamplifier attached to the multi-axis diffractometer. The electrical output signal of the scintillation detector was amplified by the preamplifier and then counted by the pulse processor.

We investigated the dependence of the count rate of signals on the incident X-ray intensity to estimate the detector deadtime. The X-ray energy was 12.398 keV. The discriminator range of the pulse processor was set to 0.21–1.50 V. An elastic X-ray scattering from a Au foil was measured in this experiment. The incident X-ray intensity was monitored using an ion chamber set at the upstream side of the diffractometer. This intensity was controlled by changing the thickness of attenuators (Al foil) located upstream of the ion

chamber. Figure 2 shows the output count rate using the $LaBr_3:Ce^{3+}$ scintillator as a function of the input count rate. The deadtime was calculated as described in a previous report [1]. The results indicated that the deadtime (τ) was 39.59 ns, which was shorter than that of the previous measurement system using a NaI:Tl scintillator (τ = 4220 ns). This shows that the count rate of the new system was intrinsically higher than that of the conventional system we have used.

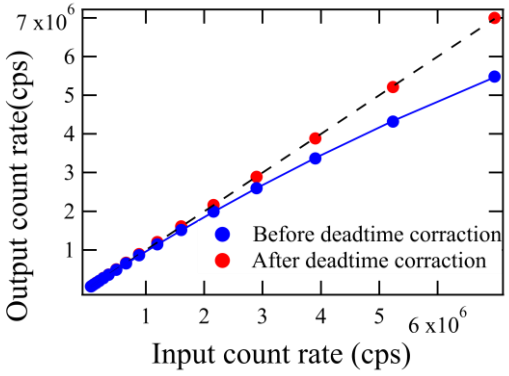

Fig. 2. Typical count rate characteristics of a $LaBr_3:Ce^{3+}$ scintillator, preamplifier, and pulse processor.

3. Significant improvement of X-ray intensity of USAXS measurement

The combination of SAXS and USAXS setups enables us to observe small-angle X-ray scattering profiles in a wide q range [2]. In particular, the data of USAXS profiles covering q less than 0.01 nm^{-1} are useful for understanding submicron-scale structures. In the early days when the SAXS apparatus was started to be used, it was difficult for the USAX setup to utilize focused X-rays because the parasitic diffuse scattering due to the mirror surfaces, which was used for focusing X-rays, affected the USAXS profile data. In FY2012, the second mirror was changed to a horizontal focus mirror in order to improve the efficiency of data collection in the SAXS setup [3, 4]. At this time, the USAXS setup was left unchanged because we did not have enough time to investigate the effect of the new mirror on the USAXS profiles. Therefore, the exposure time for USAXS was 2–3 minutes to more than 10 minutes, whereas that for SAXS was on the order of seconds. In FY2021, we investigated in detail the effect of the mirror on USAXS profile data and optimized the new optical setup for the utilization of focused X-rays in the USAXS setup, as shown in Fig. 3. As a result, the removal of the four-quadrant slit (S2) in EH2 was effective in reducing the background scattering, and an appropriate guard aperture (GA) was installed.

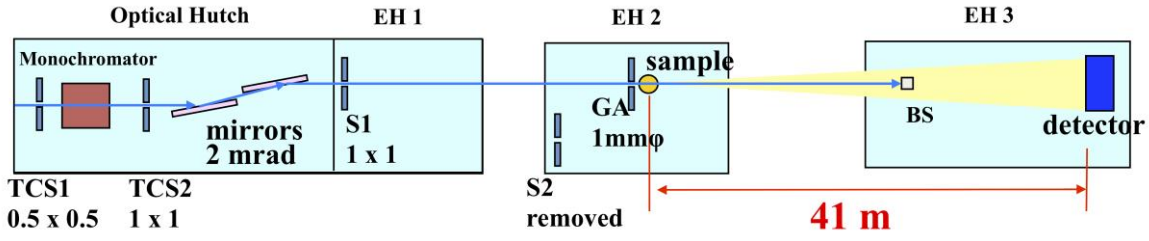

Fig. 3. Optimized setup for USAXS measurement in BL19B2. TCS: transfer channel slit, S: four-quadrant slit, EH: experimental hutch, GA: guard aperture, and BS: beam stopper. The unit of slit aperture is millimeters.

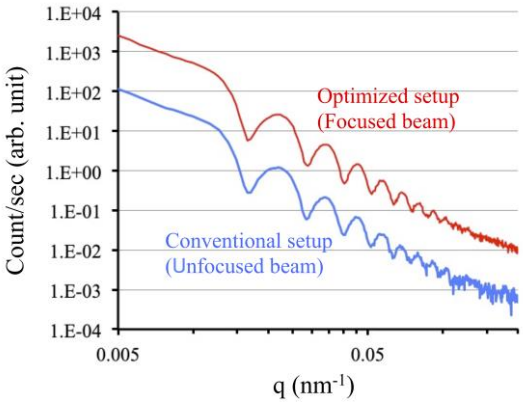

Fig. 4. USAXS profiles of spherical particles of SiO_2.

Figure 4 shows the USAXS profiles of spherical particles of SiO_2 with an average diameter of about 500 μm. The scattering intensity measured in the optimized setup with a focused beam (red) is about 22 times higher than that of the conventional unfocused setup (blue), and the efficiency of data collection of USAXS was significantly improved.

4. Temperature control device for SAXS/USAXS experiment

To meet users' demands to control the sample environment, we installed a temperature control device (HCS-302, Instec Inc.), as shown in Fig. 5. It can be set on an XZ motorized stage, and capillaries and conventional solution cells can be used for holding samples by providing some attachments. The temperature range is from –190 to 400°C, and liquid nitrogen cooling is used to achieve a quick change in sample temperature.

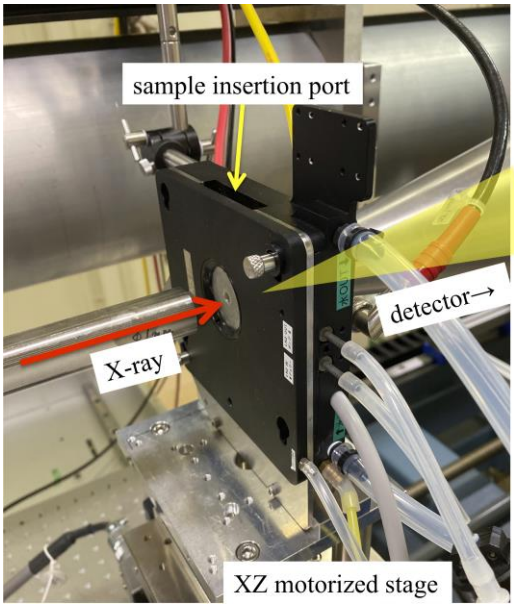

Fig. 5. Temperature control device for SAXS/USAXS experiment in BL19B2.

Osaka Keiichi and Watanabe Takeshi
Industrial Application and Partnership Division, JASRI

References:

[1] Yasuno, S. Koganezawa, T. & Kajiwara, K. (2019). *SPring-8/SACLA Annual Report FY2018*, 86–88.

[2] Osaka, K. Watanabe, T. & Sato, M. (2019). *SPring-8/SACLA Annual Report FY2018*, 44-46.

[3] Sato, M. (2018). *SPring-8/SACLA Research Reports* **6**, 234–236.

[4] Sato, M. (2018). *SPring-8/SACLA Research Reports* **6**, 245–249.